

Dynamics of Loose Materials and Oscillations of Cylindrical Perforated Sifting Surfaces with Volumetric Riffles

Serhii Kharchenko^{1*}, Sylwester Samborski¹, Farida Kharchenko²,
Izabela Korzec-Strzałka¹, Stelmakh Andrii²

¹ Lublin University of Technology, 36 Nadbystrzycka Str., Lublin, 20-618, Poland

² Sumy National Agrarian University, 160 Herasyima Kondratieva Street, Sumy, 40000, Ukraine

* Corresponding author's e-mail: s.kharchenko@pollub.pl

ABSTRACT

The application of cylindrical perforated sifting surfaces with volumetric riffles in vibrocentrifugal machines for separation of loose materials requires the development of methodologies for studying the dynamics of particles in working zones and ensuring structural reliability. The analogy with hydrodynamic models became the basis for mathematical modeling of the movement of loose materials along the sifting surface. The movement of loose material was considered as the movement of a pseudo-liquid medium, which has characteristic parameters such as viscosity, density, porosity, and layer height. The use of volumetric riffle-activators on a perforated sifting surface intensifies the processes of loose medium separating, however, it requires studying their dynamics and reliability of structures. The obtained mathematical expressions for the velocity and flow rate of the medium take into account the design and kinematic parameters of sifting surface, riffle-activators and properties of loose material. To test the obtained mathematical expressions, studies were conducted on sifting surfaces with rectangular holes with riffles of various shapes and sizes. The study also analysed the degree of properties influence of loose materials, using corn and sunflower seed mixtures as an example, on their dynamic indicators. The dynamics of loose medium on cylindrical perforated surfaces with riffle-activators is one of the main tasks for calculating the productivity and quality of the sieve separation process. Obtained appropriate dependencies of technological indicators of perforated vibrating surfaces allowed to establish ranges of variation of their rational ranges of design parameters, including the parameters of riffle-activators. The natural frequencies and shapes have been determined on the basis of numerical and experimental methods, which make it possible to assess the possibility of resonant modes during the operation of cylindrical sifting surfaces. Oscillations depending on its structural and kinematic parameters and properties of loose materials have been studied, which will ensure the reliability and technological durability of the structure of riffled sifting surfaces.

Keywords: sifting surfaces, dynamics, loose material, hole, volumetric riffle, efficiency, durability

INTRODUCTION

Separation of loose materials (LM) using perforated sifting surfaces (PSS) has found wide application in various industries [1-3]: mining, construction, chemical, medicine, agriculture, etc. PSS has been widely used in agriculture for cleaning, separation and calibration of grain materials of agricultural crops [1, 4]. Such processes are carried out on separators that have vibrating PPS of different shapes [4-6]: flat, cylindrical

and conical. The characteristic features of operating (PSS) include their insufficient specific load or productivity, which is limited by the intensity of sifting components of LM through the holes. LM properties have an influence on the separation processes. Thus, the dimensional characteristics and specific weight of agricultural crop seeds not only affect the productivity of machines, but also are quality indicators in yield level or the value of realisation of the biological potential of seeds [7-10]. It has been established that the

size of corn seeds, soybeans, sunflower and other crops affects germination, energy of seed material germination, and technological parameters in processing. For example, sowing small fractions of corn seeds reduces yield by 10-15%, which requires an increase in sowing rates [7]. The size of sunflower seeds is a significant factor in the technological processes of subsequent processing equipment, which determine the quality of products. Therefore, dimensional and typical seeding characteristics are regulated by corresponding international standards ISO.

The application of cylindrical PSS on vertical vibrocentrifugal separators is one of the ways to intensify the process of separation of LM [5, 11]. The use of vibrocentrifugal separators with cylindrical perforated rotating surfaces has proven its high specific productivity in the process of separating bulk materials in practice. Thus, the specific productivity of cylindrical PSS on a vibrocentrifugal separator is 8...12 t/m²·h, which is 3-5 times higher than the productivity of flat PSS [12, 13]. This can be explained by the additional intensive effect of a complex of forces on a particle of LM: gravity, friction, centrifugal forces.

One of the promising ways to further increase the efficiency of vibrocentrifugal separation process of LM is the use of vibrating sieves with activators [6, 14] or intensifiers [15]. This allows for a significant intensification of the processes of separating components of bulk materials while minimizing changes to the design of separation machines.

Insufficient use of the separation potential on cylindrical PSS is also due to the variable properties of LM. For example, the presence of complex shapes of agricultural crop seeds, which differ from the regular geometric shapes of PSS holes, leads to a significant reduction in the quality of separation. Compared to the separation of wheat material (an ideal case), the productivity is reduced by a correction factor when separating seeds of other crops such as buckwheat, corn, sunflower, and others [16].

Significant influence on the dynamics of particles of bulk media have kinematic and design parameters of cylindrical sieves [17], which are significant in the separation process and require consideration in the analytical analysis.

Thus, modeling of movement processes of LM on cylindrical PSS of vibrating centrifugal machines, which will comprehensively take into account the presence and parameters of

volumetric riffles, as well as the properties of seeds, is an actual task.

On the positive side for sifting is the vibration, which must be taken into account, on the other side it is a negative factor for the reliability of the perforated surfaces. This direction can be investigated analytically and experimentally [18] or with the finite element method (FEM) [19].

Moreover, in the future they are planned NDT (non-destructive) studies of sieves for increasing efficiency and productivity screening [20, 21].

The next significant factor in the effective use of cylindrical PSS in technological processes is their reliability. During operation, a number of external loads are applied to PSS [22-24]: dynamic loads from hole cleaners, inertial loads due to vibrating oscillation of sieves, load from distributed LM. This results in variable deflections of the surfaces, which serve as a source of additional disturbance for the layer of LM and determine the dynamic deformation of PSS.

PSS is a mechanical system that, due to its operational characteristics, can be subjected to resonance in the form of ratios between the natural frequencies of the system and the frequencies of external loads. Therefore, one of the tasks of studying the effectiveness of PSS is to determine the natural frequencies and shapes that allow assessing the possibility of resonance modes occurring. Studying the oscillations of PSS depending on their structural and kinematic parameters and properties of LM will ensure the reliability and technological durability of the structure

Solving the tasks will increase the efficiency of separation processes of LM on PSS, at the stages of design and operation of separating machines and calibrators.

RESEARCH METHODOLOGY

The process of separating or segregating components of LM on PSS includes the following technological stages: particle movement along the working surface; redistribution of particles within the material layer; sifting of some particles through the sieve holes; descent of material particles from PSS; cleaning of PSS holes.

The process of vibrating sieve separation or division of components of bulk materials includes the following technological steps: movement of particles on the working surface; redistribution of particles in the material layer; sifting part of the

particles through holes; sieve; cleaning of sieve holes. The intensity of these operations determines productivity and quality of separation process, and subsequently – efficiency of machines and equipment.

The use of volumetric elements in the form of welded wires, stamped ruffles and recesses on sifting perforated vibrating surfaces has been proven effective in a number of studies (Fig. 1) [6, 15, 25]. Such elements report impacts into LM and loosen them. In addition, when interacting with the ruffles, the particles rotate around their longitudinal axis, which further increases their mobility and the number of attempts to pass through the holes with their various sides. This intensifies sifting and increases the productivity of separation machines. However, the ruffle elements given in the studies have a certain round cross-sectional shape, and there are no studies of other shapes.

The dynamics of a particle of LM, which makes a complex motion along cylindrical PSS, is determined by the magnitude of displacement, velocity and acceleration. The nature of the motion of the material particle determines the quality and productivity of the separation equipment. Therefore, the solution of the problem of material dynamics is directly related to sifting processes.

Some characteristic modes of vibration lead to the fact that LM behaves like a liquid with a viscosity coefficient that depends significantly from oscillation parameters. It should be noted that the “liquefaction” of material under vibration is purely mechanical phenomenon and not a result of changes in the physical properties of the medium. When the vibrations stop, the “liquefaction” effect instantly disappears. Based on the effect of “liquefaction” of LM under vibration, researchers [6, 11, 26, 27] used the equation of motion of a

viscous fluid to determine the parameters of LM layer movement. Models of viscous fluids allow for the study of segregation and sifting of particles through PSS holes that differ in size or density. An essential advantage of using this analogy is the accounting for the interaction of dispersed particles with each other, for example, compared to modeling tasks of the material point dynamics.

In the loading mode of cylindrical PSS, the height of the LM layer shall not exceed two equivalent particle diameters. Such a mode is typical, for example, for calibrating agricultural crop seed material [4]. Then modeling the separation of such material components can be conducted based on the model of fluidised loose medium, which possesses viscosity. In the case of the movement of a thick annular grain layer on cylindrical PSS, the variability of the dynamic viscosity coefficient across the layer thickness should be taken into account, which is beyond the scope of the considered problem.

Note that the hydrodynamic model of LM motion with a constant viscosity coefficient is developed in [5, 11]. In contrast to these works, here we propose a different formulation and solution of the boundary problem, in which the influence of holes and ruffles of cylindrical PSS on the process of LM movement is taken into account.

From the point of view of oscillation theory and reliability, the design of cylindrical PSS represents a perforated thin shell of round cross-section [28, 29]. Considering the manufacturing and assembly technology, cylindrical PSS consists of two halves connected to each other and rotating around a vertical axis. The longitudinal plane of the connector is diametrical. The semi-cylinders oriented along the forming edges are bent and, after joining with an elastic layer, form

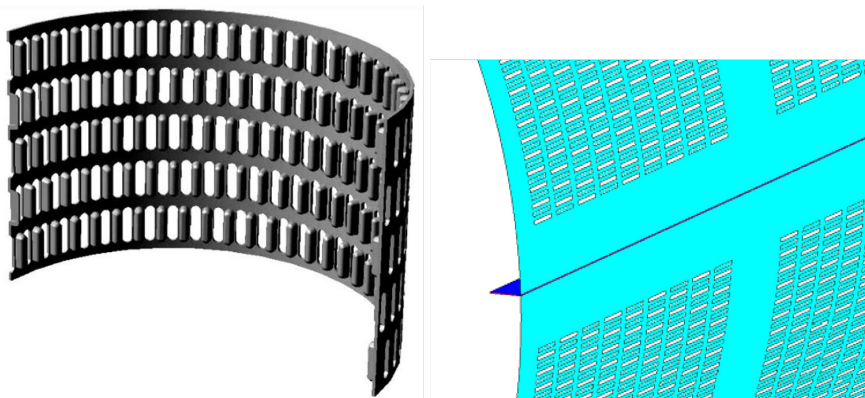


Fig. 1. Perforated sifting surfaces with volumetric ruffles

two longitudinal stiffeners (“sandwich” type) on the inner surface of the shell (Fig. 1). The elastic layer simulates the properties of real structural elements that hold the halves of the canvas together.

Cylindrical PSS have holes of various shapes (round, rectangular or triangular) and sizes, which are arranged in increments along the circumference of the cylinder and along the cylinder’s core. For the studies, a PSS was chosen, on the inner surface of which stamped ruffles were arranged between the holes. Vibrations of perforated surfaces refer to mechanical vibrations of the plates, and we consider the presence of corrugations as stiffeners. Such structures have a complex analytical solution taking into account the multiplicity of elements.

Taking into account the structural and kinematic features of PSS, the following force factors are considered for oscillation studies:

- centrifugal forces caused by the rotation of cylindrical PSS around its axis;
- forces of inertia caused by linear accelerations due to movements of PSS along its axis (reciprocating motion of the drum);
- the force effect of the cleaners;
- the effect of the LM mass on the shell during its translational and rotational motion.

For solving such problems related to PSS oscillations, the use of FEM [19, 28, 30] is effective, which allows to study the behaviour of components of complex mechanical systems under the action of various external influences.

PSS is modeled as a structure consisting of a significant number of simple entities (finite elements (FE)), within which the law of variation of sought quantities (displacements, stresses) is known and determined by the parameter values at the mesh nodes. This allows to pass from a system with an infinite number of degrees of freedom to a system with a finite number of them. In this case, all specified loads, geometric and physical characteristics, as well as initial deformations are reduced to nodes. The implementation of the method allows determining the stress-strain state at any point of PSS.

We use the following algorithm: building the functional; decomposing the system into FE and selecting coordinate functions; constructing stiffness and mass matrices, bringing distributed loads to nodes for each FE; formulating and solving canonical equations.

The aim of the study is to develop a methodology for determining the dynamic parameters

Table 1. Structural and kinematic parameters of PSS of vibrocentrifugal separators (BCS)

Parameters	Designations	Values
Radius, m	R_R	0.3075
Length, m	L	0.5
Angular velocity, rad/s (s^{-1})	ω	11.77
Frequency of vertical oscillations, s^{-1}	n	75.9
Amplitude of vertical oscillations, m	A	0.008
Area, m^2	S_{ps}	0.97

(velocity and volumetric flow rate) of LM during its sifting and the natural frequencies of oscillations of cylindrical PSS with ruffles, which takes into account the design parameters of PSS, vibration parameters, properties of LM.

MATERIALS

Corn and sunflower grains are used as LM. Their physical and mechanical properties, which are necessary for calculations, are taken from known studies [31, 32] or obtained experimentally.

Structural and kinematic parameters of cylindrical PSS are accepted in accordance with the characteristics of a serial separator of BCS type (SVS-15, A1-BCS-25, R8-BCS, R8-UZK-25, B1-VCS) (Table 1), accepted according to [5, 33, 34].

Cylindrical PSS consisting of two halves in basic (without ruffles) and proposed (ruffled) design (Fig. 2) were used for the research.

Parameters of PSS holes and ruffles are accepted for LM of corn and sunflower (Table 2). The data on the parameters of holes were taken in accordance with the capabilities of the industrial manufacturer [35], based on the serial cold stamping of perforated steel sheets. To minimize

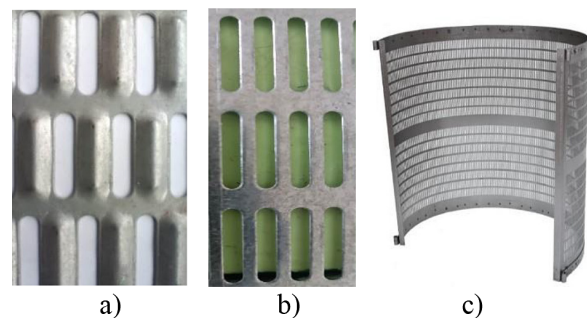


Fig. 2. Samples of perforated sifting surfaces: (a) ruffled; (b) basic (nonruffled); (c) half of cylindrical surface

Table 2. Technological parameters of PSS of accepted loose materials

Parameters	Designations	Type of loose material	
		corn	sunflower
Hole width, m	b_h	0.004	0.0024
Hole length, m	l_h	0.025	0.02
PSS hole area, 10^{-4} m^2	S_0	1	0.48
Number of holes, pcs	N_0	1736	4314
Number of ruffles, pcs	N_r	1736	4314
Riffle width, 10^{-3} m	b_r	4	3
Riffle height, 10^{-3} m	h_r	1–5	1–3

the reduction of the “live” cross-sectional area of PSS, the width of ruffles is matched to hole width and is a fixed parameter. In the studies, the height of ruffles was varied taking into account the technological possibilities of practical manufacturing of such PSS. Parameters of ruffles with different cross-sectional shapes are presented in Table 2.

METHODS

Study of the dynamics of loose materials during their sifting

The use of volumetric ruffles on PSS of vibrating centrifugal sieves (Fig. 3) leads to a complex effect on the particles of loose material. On the one hand, the particles of the material are oriented towards the holes by being lifted on the ruffles. At the same time, the rotation of the particles leads to impulses in the layer of material, which increases the number of pores, the mobility of the particles and has a positive effect on their sifting through the holes [15].

However, the arrangement of ruffles on the working surface of the vibrating PSS creates additional resistance to the movement of LM particles. Part of the material particles, which by size does not pass into the holes, moves and constantly receives resistance to movement from the installed ruffles. It should be noted that the amount of resistance to movement will be influenced by: parameters of the ruffles, kinematic parameters of the vibrating PSS, properties of seed material. This requires a separate study and appropriate research.

Ruffles (Fig. 3) have a volumetric longitudinal (relative to the axis of material movement) design. They are located in place of part of the

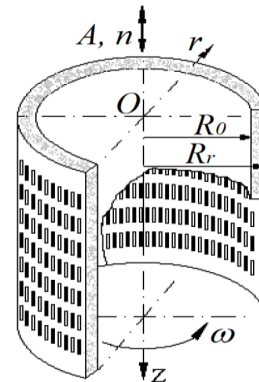


Fig. 3. Scheme of cylindrical perforated sifting surface with volumetric ruffles

holes and displaced in rows. The checkerboard arrangement of ruffles provides multiple impacts (orientation) on particles of LM.

Components of LM, moving along the PSS, fall on longitudinal volumetric ruffles-activators. The ruffles rotate the loose medium particle around its longitudinal axis and orient it into the elongated hole according to the separating parameter – thickness.

Let’s conduct theoretical research on the movement of particles of LM on a similar riffled cylindrical PSS. Modeling the movement of seed material along the internal working surface of a vertical cylindrical PSS using the hydrodynamic analogy requires consideration of a homogeneous liquid with a specific viscosity [5, 36].

The vibration viscosity coefficient of fluidized medium under the vibration depends on the centrifugal force. To study the magnitude of the vibroviscosity coefficient, it is necessary to consider the distance of coordinate r (Fig. 3) of the annular layer from the rotational axis of cylindrical vibrating PSS. The task in hydrodynamics is to investigate an heterogeneous pseudo-liquid, where viscosity increases as it approaches the surface of cylindrical PSS.

The difference from the known researches is the necessity to take into account the degree of influence of parameters of holes and volumetric ruffles on the dynamics of LM particles on the operating PSS. LM moves along inner PSS with R_r radius by annular layer of thickness h (Fig. 3). The velocity of LM $U(r)$ is directed along the z -axis and depends on the radial coordinate r . The upper boundary of the medium layer is located at a distance $R_0=R_r-h$. Cylindrical PSS rotates around the z -axis with an angular velocity of ω and performs vertical oscillations along it with an amplitude A and a frequency n (Fig. 3).

Assuming a constant dynamic viscosity coefficient, the velocity of the fluidised medium is the solution of the equation [37]:

$$\frac{d^2U}{dr^2} + \frac{1}{r} \frac{dU}{dr} = N, \tag{1}$$

in which

$$N = -\frac{1}{\mu} \left(\frac{\Delta P}{l} + \rho g \right), \tag{2}$$

where: $\Delta P/l$ – change in pressure relative to the height of fluidized medium layer that moves along PSS; ρ – density of LM layer.

The dynamic viscosity coefficient of the medium layer is determined by the expression found in [38]:

$$\mu = \frac{F_T}{6nd \sqrt{(A)^2 - \left(\frac{\pi F_T}{2m\gamma n^2} \right)^2}}, \tag{3}$$

where: $F_T = \frac{f\pi^2 d^2 p \xi}{4}$ – friction force acting on the particle at medium oscillations; d, m – averaged values of diameter and mass of one particle of LM; γ – mass attachment coefficient to a moving particle of the material; $p = \frac{\rho \omega^2}{2} \left(\left(R_R - \frac{h}{2} \right)^2 - R_0^2 \right)$ – internal pressure in LM from [5]; f – coefficient of internal dry friction of medium particles; ξ – correction coefficient, which takes into account the porosity of the medium.

We will define boundary conditions that characterize the course of the process and allow us to solve equations (2). There are no tangential stresses on the inner surface of the moving LM layer $r = R_0 = R_R - h$, so accept:

$$\frac{dU}{dr} = 0. \tag{4}$$

On the PSS $r = R_R$ there is an interaction force between LM and PSS – the dry friction force, which is considered independent of the speed $U(R_R)$. It corresponds to the average tangential stress:

$$\tau_1 = f_0 p_1 (1 - \varepsilon), \tag{5}$$

where: $p_1 = \rho h R_R \omega^2$ – pressure in the medium at cylindrical PSS; f_0 – dynamic coefficient of friction of LM particles on cylindrical PSS; ε – free area ratio of the PSS, which is determined according to the following formula:

$$\varepsilon = \frac{\sum S_0}{S} 100\% = \frac{N_0 S_0}{2\pi R_R L} \cdot 100\%, \tag{6}$$

where: S_0 – is the area of one hole of PSS; S – total surface area of PSS; N_0 – number of holes in PSS; L – length of PSS (cylinder height).

Taking into account the transformations, we have:

$$\tau_1 = f_0 \rho h R_R \omega^2 \left(1 - \frac{N_0 S_0}{2\pi R_R L} \right) = \frac{f_0 \rho h \omega^2}{2\pi L} (2\pi R_R L - N_0 S_0). \tag{7}$$

On PSS there is also an interaction of the moving layer of the medium with volumetric ruffles and holes between them. The force of action of one ruffle is taken proportional to the area of its cross-section, pressure p_1 and the first degree of fraction velocity, i.e. in the form of:

$$F_r = K S_r p_1 U(r), \tag{8}$$

where: S_r – cross-sectional area of the ruffle; K – corrugation coefficient which takes into account the interaction between the ruffle and LM.

For calculations, we accept several variants of ruffles (Fig. 4): with rectangular cross-section:

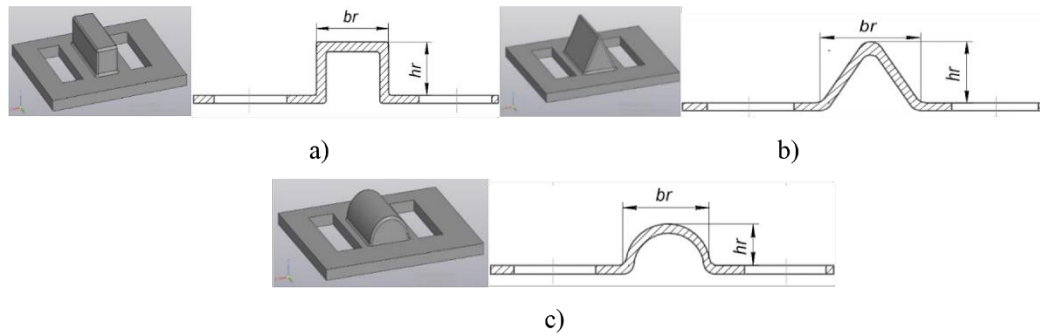


Fig. 4. Variants of volumetric ruffles with different cross-section: (a) rectangular; (b) triangular; (c) as a semicircle

$S_{rr} = h_r b_r$, where h_r, b_r – is the ruffle height and width; with triangular cross-section: $S_{rr} = \frac{1}{2} b_r h_r$; with a semicircle cross-section: $S_{rr} = \frac{\pi b_r^2}{8}$, where $h_r = b_r / 2$.

Force (8) corresponds to the average tangential stress:

$$\tau_2 = \frac{F_r}{S} = \frac{KS_r N_r \rho_1 U(r)}{S} = \frac{KS_r \rho h \omega^2 N_r U(r)}{2\pi L}, \tag{9}$$

where: N_r – is the number of ruffles on the PSS; S_r – ruffle cross-sectional area.

We will form a second boundary condition at $r = R_R$:

$$-\mu \frac{dU}{dr} = \tau_1 + \tau_2. \tag{10}$$

We emphasize that in (10) $\tau_2 > 0$. At $\tau_2 = 0$ the stated formulation of the boundary value problem loses its correctness.

The general solution (1) is the sum

$$U(r) = \frac{1}{4} N r^2 + c_1 \ln r + c_2, \tag{11}$$

where: c_1 and c_2 – is the arbitrary constants. Their values are determined using the boundary conditions (4), (10). The first of these is performed at

$$c_1 = -\frac{1}{2} N R_0^2. \tag{12}$$

The second boundary condition is satisfied when:

$$c_2 = -\frac{\mu N \pi L}{KS_r \rho R_R \omega^2 N_r} R_0 - \frac{N R_R^2}{4} - c_1 \ln R_R - \frac{f_0 (2\pi R_R L - N_0 S_0)}{KS_r N_r}. \tag{13}$$

Considering the solution (11) and values of constants (12), (13), we obtain the expression for the velocity of LM on cylindrical PSS:

$$U(r) = \frac{1}{4} N r^2 - \frac{N R_0^2}{2} \ln r - \frac{\mu N \pi L (R_R - h)}{KS_r \rho R_R \omega^2 N_r} - \frac{1}{4} N R_R^2 + \frac{N R_0^2}{2} \ln R_R - \frac{f_0 (2\pi R_R L - N_0 S_0)}{KS_r N_r}$$

Or convert to:

$$U(r) = \frac{N}{2} \left[\frac{r^2 - R_R^2}{2} + R_0^2 \ln \frac{R_R}{r} - \frac{2\mu \pi L R_0}{KS_r \rho R_R \omega^2 N_r} - \frac{2f_0 (2\pi R_R L - N_0 S_0)}{NKS_r N_r} \right]. \tag{14}$$

The volumetric flow rate (separator capacity) of LM is found by integrating:

$$Q = 2\pi \int_{R_0}^{R_R} r U(r) dr. \tag{15}$$

Calculating the integral, taking into account $R_0 = R_R - h$ results in the formula:

$$Q = \frac{\pi N}{2} \left\{ (R_0 h + h^2) \left[\frac{3R_0^2 - R_R^2}{4} - \frac{2\mu \pi L R_0}{KS_r \rho R_R \omega^2 N_r} - \frac{2f_0 (2\pi R_R L - N_0 S_0)}{NKS_r N_r} \right] + R_0^4 \ln \frac{R_0}{R_R} \right\}. \tag{16}$$

Since in the considered problem $h \ll R_R$, neglecting the small terms, instead of (16) we get a simpler approximate mathematical expression for productivity of cylindrical PSS:

$$Q \approx -2\pi R_R h N \left[\frac{h^2}{3} + \frac{2\pi L \mu}{K S_r \rho \omega^2 N_r} + \frac{f_0 (2\pi R_R L - N_0 S_0)}{N K S_r} \right]. \quad (17)$$

Productivity of PSS is also determined from the expression:

$$Q = u_{cp} S_k = u_{cp} 2\pi R_R h, \quad (18)$$

where: S_k – is the annular area of LM which moves inside PSS.

Then, the average speed of movement of the descent fraction:

$$U_{cp} = \frac{Q}{2\pi R_R h} = -N \left[\frac{h^2}{3} + \frac{2\pi L \mu}{K S_r \rho \omega^2 N_r} + \frac{f_0 (2\pi R_R L - N_0 S_0)}{N K S_r} \right]. \quad (19)$$

In the case when $\Delta p = 0$ convert (2) and have $N = -\frac{\rho g}{\mu}$.

Then, the dependence (17) is converted into a finite mathematical expression for productivity of cylindrical PSS:

$$\begin{aligned} Q &= -2\pi R_R h \left(-\frac{\rho g}{\mu} \right) \left[\frac{h^2}{3} + \frac{2\pi L \mu}{K S_r \rho \omega^2 N_r} - \left(\frac{f_0 (2\pi R_R L - N_0 S_0) \mu}{\rho g K S_r} \right) \right] = \\ &= 2\pi R_R h \left[\frac{h^2 \rho g}{3\mu} + \frac{1}{K S_r} \left(\frac{2\pi L g}{\omega^2 N_r} - f_0 (2\pi R_R L - N_0 S_0) \right) \right]. \end{aligned} \quad (20)$$

The dependence (19) is also converted into a finite mathematical expression for the average velocity of LM on cylindrical PSS:

$$\begin{aligned} U_{cp} &= - \left(-\frac{\rho g}{\mu} \right) \left[\frac{h^2}{3} + \frac{2\pi L \mu}{K S_r \rho \omega^2 N_r} - \left(\frac{f_0 (2\pi R_R L - N_0 S_0) \mu}{\rho g K S_r} \right) \right] = \\ &= \frac{h^2 \rho g}{3\mu} + \frac{1}{K S_r} \left(\frac{2\pi L g}{\omega^2 N_r} - f_0 (2\pi R_R L - N_0 S_0) \right). \end{aligned} \quad (21)$$

Thus, equations (20), (21) and (3) are the final mathematical expressions for determining the parameters of LM dynamics and productivity of cylindrical PSS, taking into account the variability of volumetric activator parameters.

Experimental studies of loose material dynamics

For experimental studies of the movement of particles of bulk materials on one of the two components of cylindrical PSS, along the generatrix, a stepped-shaped bend 1 (Fig. 5) was made. A rectangular opening is cut into the wall 2 of the step, and acrylic glass 3 with a coordinate grid is inserted.

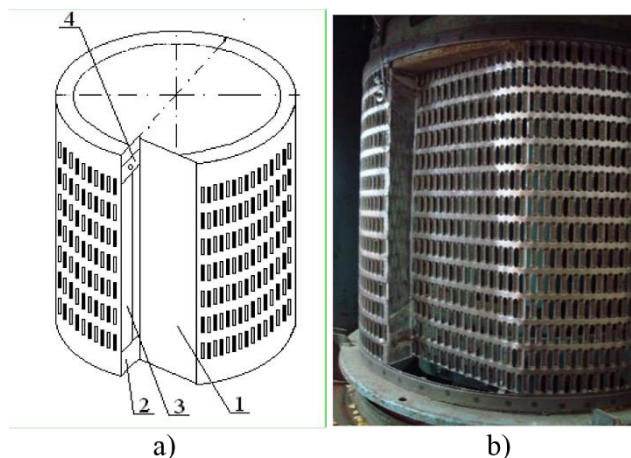


Fig. 5. Cylindrical perforated sifting surface with stepped longitudinal bending: (a) diagram: 1 – stepped bending; 2 – radial step wall; 3 – plexiglass; 4 – device for input of labelled particles; (b) general view

The study of the displacement of individual colored particles in a LM layer was conducted using a high-speed camera Phantom V9.1 (14-bit image depth, 1000 frames/s, resolution of 1632×1200 pixels, color). The processing of the obtained images was carried out by tracking the path of colored particles. The distances travelled by the coloured particles and their velocities became known as a result of determining the coordinates of the particles in the video frames and the frequency of frame changes per unit time. By measuring the distance L_p , traveled by the colored particle of LM over a period of time, we determined its velocity:

$$v_{ek} = L_p / t_k k_k, \tag{22}$$

where: k – number of frames corresponding to the displacement of the particle over a distance L_p , $t_k=1/n$ – single frame time, n – frame rate per second.

Using the obtained velocity, the volumetric flow rate of LM was determined by PSS using the expression (18).

Studies of the natural frequencies and oscillation modes of cylindrical PSS

Numerical studies

The accuracy of modeling using FEM depends on: the adequacy of the assumptions made regarding the operating conditions of PSS structure, the selected type of finite elements, their shape and quantity. The response of cylindrical PSS to a combination of external influences can be reduced to a spatial problem of deformable solid mechanics [39]:

$$\sigma_{ij} + f_i^* = 0, i=1,2,3; \quad \sigma_{ij} = C_{ijkl}\varepsilon_{kl}, i,j,k,l=1,2,3; \quad 2\varepsilon_{ij} = u_{ij} + u_{ji}, i,j=1,2,3, \tag{23}$$

where: u_{ij} – elements of the displacement vector of the points of the investigated elements in the Cartesian coordinate system x_k ; $\sigma_{ij}, \varepsilon_{kl}, C_{ijkl}$ – tension tensors, strains and elastic constants of materials, respectively; f_i^* – mass forces.

Solving equation (23) requires introducing a system of initial and boundary conditions, as well as representing of PSS as a thin-walled structure (a combination of beams, plates, and shells). In the finite element formulation in nodal displacements V , the resolving system of equations takes the following form for dynamic impact problems [40, 41]:

$$M\ddot{V} + K\dot{V} + CV = P_v(t), \tag{24}$$

where: M, C, K – matrix of mass, stiffness and damping of the studied sieve cloth; P_v – vector of external loads, brought to the nodes of the finite element mesh.

For the problem of free oscillations of a sieve cloth, when there is no external disturbance ($P_v(t))=0$ and there is stationarity of the action functional, the resolving system of equations will take the form:

$$M\ddot{V} + CV = 0. \tag{25}$$

with a solution $V = \Lambda_k \sin(\omega_k t + \alpha)$.

Differential equations (25) are transformed into a system of homogeneous linear algebraic equations:

$$(C - M\omega_k^2)\Lambda_k = 0, \tag{26}$$

where: ω_k^2 – square of the natural frequency, Λ_k – eigenform vector.

Transform (26) by taking $\omega_k^2 = p$ and transfer p and C :

$$C^{-1}M\Lambda_k = p^{-1}\Lambda_k, \tag{27}$$

or $Q^* = C^{-1}M, \lambda = p^{-1},$

where: Q^*, λ – matrix and its eigenvalues.

In this case, the matrix Q^* is not symmetrical. Otherwise, it can be obtained as the result of multiplying three matrices: $Q^* = L^{-1}CL^T$, and the triangular matrix L is the result of decomposition of the Cholesky matrix M , so that $M = LL^T$. The matrix obtained in this way Q^* is symmetrical [42]. The eigenvalues λ , being real due to the symmetry of the matrices M, C and the positive definiteness of the matrix M , represent, in the first case, quantities that are inversely proportional to the squares of the natural frequencies of the considered mechanical system, and in the second case, they represent the squares of the frequencies. The eigenvectors in the first variant coincide with the vectors Λ_k .

The system of equations (24) will be integrated by the Newton-Raphson method. At the same time, the vector $P_v(t)$ of the right parts, which defines the external disturbance, is calculated at each step of integration.

Cylindrical PSS as an object of FEM modeling creates difficulties that are associated with design features: the presence of a significant number of rectangular holes (25% of the total area) and volumetric ruffles, stress concentrators near the holes, etc. Let's imagine PSS in the form of a plate-shell-beam structure and take into account the stress-strain state of these elements, which are described by the structural stiffness matrix, the mass matrix, the nodal load array, etc.

To create a FEM of cylindrical PSS used software ANSYS. The initial stage involved analyzing the geometry of PSS and selecting FE to describe its shape and the physical and mechanical processes of elastic deformation. For modeling, ANSYS library FE systems of the following types were used: massive (SOLID187), plate-shell (SHELL63), and beam (BEAM4). This made it

possible to obtain a model of cylindrical PSS with ruffles and rectangular holes in the form of plate-shell-beam structure, which contains about 165 thousand nodes and 273 thousand FE. Further increase in nodes and FE increases the time spent on calculations and slightly (up to 0.2%) changes the parameter values.

Experimental studies

For experimental measurement of frequency characteristics of components, methods based on applying sinusoidal forces to the object, slowly varying their frequency, are used. The use of harmonic excitation, which is a special case of periodic excitation, has several advantages. The investigated mechanical system responds to such excitation as a set of oscillators, especially in cases where the corresponding decrements are small, i.e., for those natural frequencies that are most important. The results of analyzing the response of structures to harmonic excitation are least affected by errors and resonance phenomena are visually apparent.

For experimental determination of the natural frequencies and shapes of PSS, a laboratory setup was used (Fig. 6).

An electromagnetic vibration exciter (Fig. 6b, pos. 7) was used to create a disturbance. Sensors with inductive transducers (Fig. 6b, pos.10) were used to measure displacements. PSS (Fig. 6b, pos.1) was fixed on the plate (Fig. 6b, pos. 2). The halves of PSS were attracted to the rings (Fig. 6b, pos. 5) and fastened together. This made it possible to simulate the installation conditions on real machines. An inductive sensor (Fig. 6b, pos. 10) is fixed on the bracket (Fig. 6b, pos. 10), which can be moved in a circumferential direction by means of an electric motor (Fig. 6b, pos. 11).

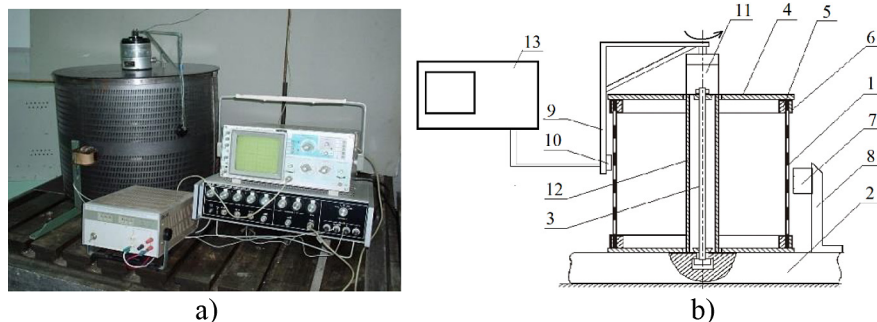


Fig. 6. Laboratory setup for determining frequencies of PSS: (a) general view; (b) scheme: 1 – PSS; 2 – slab; 3 – screed; 4 – plate; 5 – ring; 6 – belt; 7 – vibration exciter; 8,9 – brackets; 10 – sensor; 11 – electric motor; 12 – stand; 13 – oscilloscope S1-96

The disturbance was set by the signal of the low-frequency generator GZ-123, transmitted directly to the vibration exciter. PSS oscillations were recorded by a two-beam oscilloscope S1-96 (Fig. 6b, pos. 13), to which the signal of the NIR-2 displacement sensor was transmitted. Since only one rotation of the sensor is enough to record the distribution of radial displacements around the circumference of the cloth, wires from the sensor to the oscilloscope were connected without the use of a current collector.

The excitation frequency was initially set according to calculated values and then adjusted until the system entered a resonant state. By smoothly changing the frequency of the disturbance, the maximum amplitude of the curve on the oscilloscope screen was achieved and the corresponding frequency value was taken as one of the own. The error in determining the maximum amplitude does not exceed 2.5% (one grid division on the oscilloscope screen). Next, a full rotation of the sensor around PSS was performed, and the number of nodes was calculated, as well as their angular position on the circle to determine the shape of the oscillations.

The natural frequency ω_r of the system without damping corresponds to the maximum amplitude, measured by the velocity sensor (the velocity has zero phase shift φ_r relative to the driving force), while the phase shift of displacement relative to the driving force is $\pi/2$. The frequency $p_r = \omega_r$ at which $\varphi_r = 0$ for velocity oscillations is called the phase resonance frequency, and the value of $p_r < \omega_e$ (ω_e – the frequency of free oscillations of the system with damping) corresponding to the maximum displacement. When the damping decreases (at small logarithmic decrements), these values are practically the same [43].

The logarithmic decrement δ is related to the absorption coefficient ψ by the dependence [43]: $\delta = \psi/2$. In the same study, the value of the absorption coefficient for steel is provided as $\psi = 0.01-0.02$. Even assuming a tenfold increase in

the value of ψ for the actual construction, in this case, the decrement δ would be 0.05-0.10, i.e., it remains small. Therefore, determining the natural frequency based on the frequency of the amplitude resonance is well justified in this case.

RESULTS

Dynamics of loose materials

Preliminary studies have shown a significant influence of the shape of LM components on the efficiency of their sifting through holes of PSS with ruffles [4, 14]. To fully validate the adequacy of the obtained mathematical expressions, calculations were conducted for LM in the form of corn and sunflower seeds, which have distinctive properties (Table 3). The dimensions and physical properties of the loose material determine the indicators of technological productivity.

As a result of numerical simulation, graphic dependences of the dynamic viscosity coefficient of the LM medium (Fig. 7), medium velocity (Fig. 8, 9) and PSS productivity (Fig. 10) were obtained.

As a result of the research it was found (Fig. 7) that the dynamic viscosity coefficient of the medium depends on the friction coefficient and the medium layer height on PSS. This coefficient is a value that comprehensively characterizes the dynamic properties of a LM, including: size, shape, density, friction angles, etc. Similarly, the use of a complex value significantly improves parameter optimization by reducing the significant factors. The expediency of using this particular coefficient for a comprehensive assessment of the properties of the medium has been proven in many works [11, 26, 34]. The range of variation for corn LM was 0.12-0.63 Pa·s, sunflower – 0.05-0.13 Pa·s. The viscosity of the medium is a significant and generalized parameter that determines the dynamics of the medium and the productivity of PSS.

Table 3. Cross-sectional area of riffle depending on its profile and height

Parameters	Designations	Type of loose material				
		corn			sunflower	
Riffle height, 10^{-3} m	h_r	1	3	5	1	2
Cross-sectional area of riffle with rectangular profile S_{rr} , 10^{-4} m ²	S_{rr}	0.04	0.12	0.2	0.03	0.06
Cross-sectional area of riffle with triangular profile S_{rt} , 10^{-4} m ²	S_{rt}	0.02	0.06	0.1	0.015	0.03
Cross-sectional area of riffle with oval profile S_{rs} , 10^{-4} m ²	S_{rs}	0.031	0.094	0.157	0.024	0.047

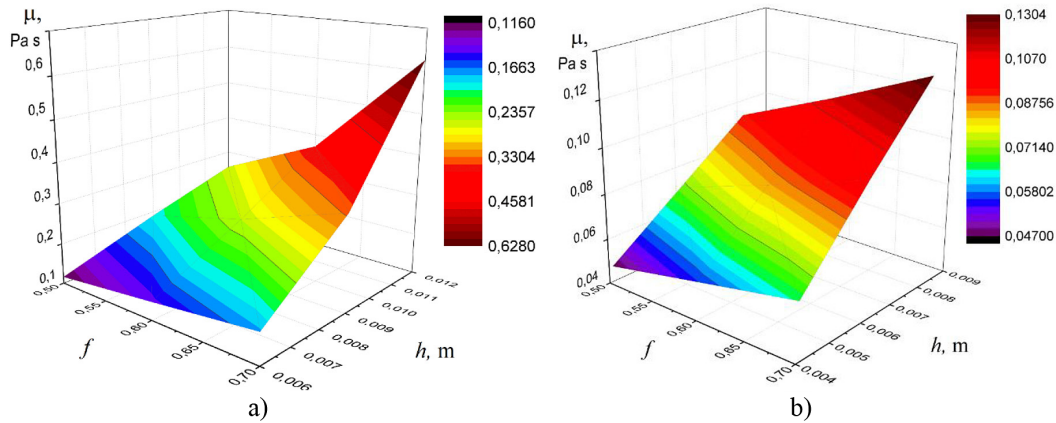


Fig. 7. Dependencies of the dynamic viscosity coefficient of the medium on the friction coefficient of particles and layer height: (a) corn LM ($A=0,008\text{m}$, $n=75,9\text{s}^{-1}$; $f_0=0,27$; $S_0=1\times 10^{-4}\text{m}^2$; $R=0,3075\text{m}$; $l=0,5\text{m}$; $b_p=0,004\text{m}$; $N_p=1736$; $K=40\text{s/m}$; $d=0,006\text{m}$; $\rho=730\text{kg/m}^3$; $\xi=0,65$); (b) sunflower LM ($A=0,008\text{m}$, $n=75,9\text{s}^{-1}$; $f_0=0,27$; $S_0=4,8\times 10^{-5}\text{m}^2$; $R=0,3075\text{m}$; $l=0,5\text{m}$; $b_p=0,003\text{m}$; $N_p=4314$; $K=40\text{s/m}$; $d=0,004\text{m}$; $\rho=390\text{kg/m}^3$; $\xi=0,65$)

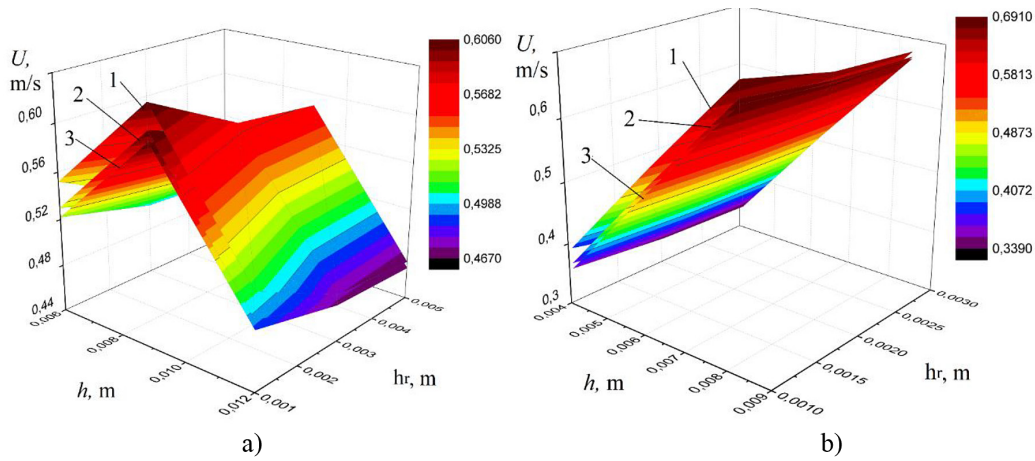


Fig. 8. Analytical dependences of medium velocity on layer height (h) and height of installed riffles (h_r) for different shapes of its profile: 1 – triangular; 2 – oval; 3 – rectangular; (a) corn LM ($A=0,008\text{m}$, $n=75,9\text{s}^{-1}$; $f=0,7$; $f_0=0,27$; $S_0=1\times 10^{-4}\text{m}^2$; $R=0,3075\text{m}$; $l=0,5\text{m}$; $b_p=0,004\text{m}$; $N_p=1736$; $K=40\text{ s/m}$; $d=0,006\text{m}$; $\rho=730\text{kg/m}^3$; $\xi=0,65$); (b) sunflower LM ($A=0,008\text{m}$, $n=75,9\text{s}^{-1}$; $f=0,7$; $f_0=0,27$; $S_0=4,8\times 10^{-5}\text{m}^2$; $R=0,3075\text{m}$; $l=0,5\text{m}$; $b_p=0,003\text{m}$; $N_p=4314$; $K=40\text{ s/m}$; $d=0,004\text{m}$; $\rho=390\text{ kg/m}^3$; $\xi=0,65$)

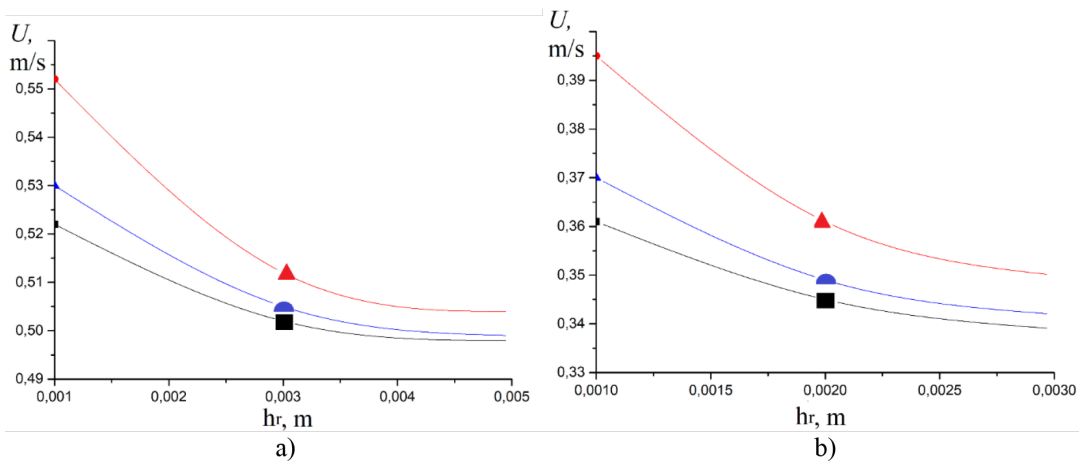


Fig. 9. Analytical dependences of medium velocity on layer height (h_r) for different shapes of its profile: ● – oval; ▲ – triangular; ■ – rectangular: (a) corn LM ($A=0,008\text{m}$, $n=75,9\text{s}^{-1}$; $f=0,7$; $f_0=0,27$; $S_0=1\times 10^{-4}\text{m}^2$; $R=0,3075\text{m}$; $l=0,5\text{m}$; $b_p=0,004\text{m}$; $N_p=1736$; $K=40\text{ s/m}$; $d=0,006\text{m}$; $\rho=730\text{ kg/m}^3$; $\xi=0,65$; $h=0,006\text{m}$); (b) sunflower LM ($A=0,008\text{m}$, $n=75,9\text{s}^{-1}$; $f=0,7$; $f_0=0,27$; $S_0=4,8\times 10^{-5}\text{m}^2$; $R=0,3075\text{m}$; $l=0,5\text{m}$; $b_p=0,003\text{m}$; $N_p=4314$; $K=40\text{ s/m}$; $d=0,004\text{m}$; $\rho=390\text{kg/m}^3$; $\xi=0,65$; $h=0,004\text{m}$)

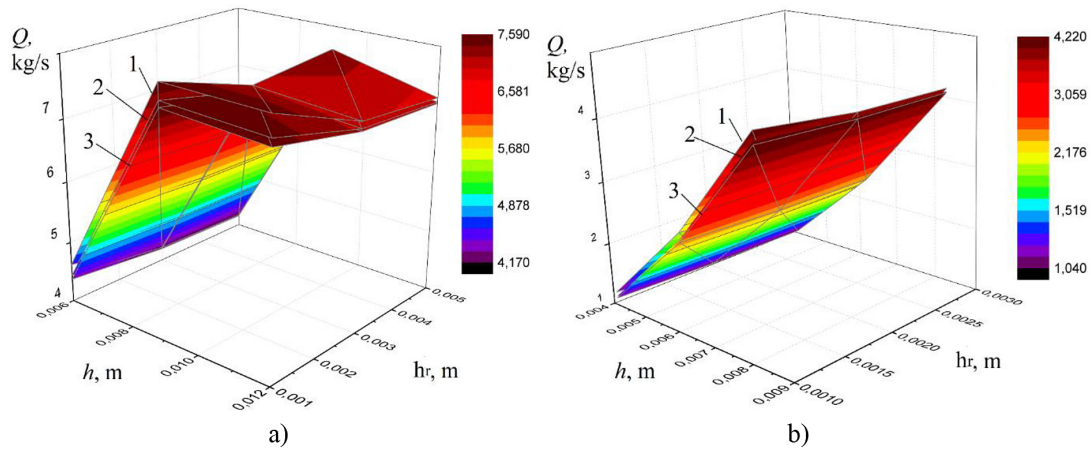


Fig. 10. Analytical dependences of productivity of cylindrical PSS on the layer height (h): at various shapes of its profile 1 – triangular; 2 – oval; 3 – rectangular; a – corn LM ($A=0,008\text{m}$, $n=75,9\text{s}^{-1}$; $f=0,7$; $f_0=0,27$; $S_0=1\times 10^{-4}\text{m}^2$; $R=0,3075\text{m}$; $l=0,5\text{m}$; $b=0,004\text{m}$; $N_p=1736$; $K=40\text{s/m}$; $d=0,006\text{m}$; $\rho=730\text{kg/m}^3$; $\xi=0,65$); b – sunflower LM ($A=0,008\text{m}$, $n=75,9\text{s}^{-1}$; $f=0,7$; $f_0=0,27$; $S_0=4,8\times 10^{-5}\text{m}^2$; $R=0,3075\text{m}$; $l=0,5\text{m}$; $b_p=0,003\text{m}$; $N_p=4314$; $K=40\text{s/m}$; $d=0,004\text{m}$; $\rho=390\text{kg/m}^3$; $\xi=0,65$).

Variation of material velocity on PSS was obtained taking into account variation of ruffles parameters and medium layer height. The ranges of variation of corn LM velocity of 0.47-0.61 m/s, sunflower 0.34-0.69 m/s were obtained.

Increasing the ruffles height, in the studied range, leads to a decrease in corn LM velocity of 4.31-8.11% to 0.5 m/s, sunflower of 5.81-10.2 % to 0.345 m/s (Fig. 8). The least influence on the decrease in velocity is exerted by ruffles with a triangular cross-sectional shape, followed by rounded and rectangular ones. The low velocity of the medium with rectangular ruffles is explained by the maximum area of their cross-section.

The analysis of dependencies (Fig. 10) established that increasing the medium layer height within the studied range increases productivity by 70.42-71.24%: to 7.92 kg/s at separation of corn LM, and by 264.3-291.6% to 4.41 kg/s at separation of sunflower LM. Such an increase in the layer of LM is typical for changing the technological mode of calibration into fractions, preliminary or primary separation. The maximum values of the productivity of PSS were obtained for a triangular cross-sectional ruffle profile, regardless of the type of medium and its layer height. The increase in productivity on PSS with these ruffles was 1.2-6% for the corn LM and 1.65-9.19% (sunflower) and compared to ruffles of rectangular and oval cross-section. The greatest difference in productivity values of PSS is observed at low ruffles height ($h_r=1\text{mm}$) – 3.5-6% (corn) 3.4-6.5% (sunflower), the lowest at $h_r=3\text{mm}$ – 1-4.5% (corn) and 1.2-3.2% (sunflower).

The mathematical expressions (3), (20), (21) and the graphical dependencies (Fig. 3-6) obtained allow for the refinement of mathematical models for modeling the processes of motion of bulk materials. This makes it possible to take into account the parameters of holes, ruffles, and generalized properties of the medium in the processes of separating its components on cylindrical PSS.

This methodology can be used for modeling the dynamics of LM on perforated surfaces with holes and ruffles of various configurations. To verify the adequacy of the obtained analytical expressions, experiments were conducted, and a comparison was made (Fig. 11).

The discrepancy between the results was up to 3.4%, which indicates the adequacy and

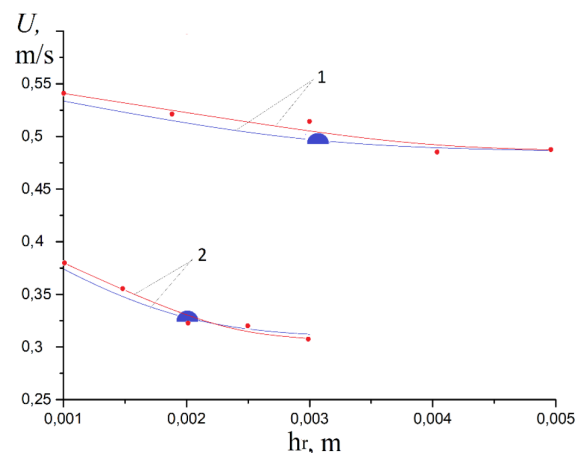


Fig.11. Dependence of loose material velocity on the ruffle height of oval profile: 1 – corn LM; 2 – sunflower LM; blue lines – analytical data; red lines – experimental data

possibility of using the mathematical expressions for modeling the dynamics of LM on PSS with holes and ruffles of various configurations.

Calculation results of oscillations of cylindrical PSS

In the results of calculations of the perforated sifting shell model, the values of the natural oscillations for different forms of oscillations were obtained (Fig. 12-14, Table 4).

Based on the actual vibration parameters of the separation equipment, the analysis was limited to eight modes. During the technological process of separation, the internal PSS is covered with a layer of LM, acting as an attached mass. To assess its influence on the dynamic characteristics of PSS, its natural frequencies and modes were also determined. The thickness of LM layer was assumed to be constant in the circumferential direction and variable along the PSS generatrix at a density of 810 kg/m³. The typically assumed value for calculations, 730 kg/m³ (for corn), increases by approximately 11% due to the action of centrifugal forces.

Analysis of the obtained frequencies and modes of the natural oscillations shows the following:

- the character of the natural modes corresponds to the provisions of the shell theory: the lowest natural modes have one half-wave along the generatrix and several half-waves in the

circumferential direction, which provides a basis for rationally choosing the number of harmonics in the decomposition of the external load by spatial coordinates while maintaining acceptable accuracy;

- the presence of ruffles increases the stiffness of the structure and raises the natural oscillation frequencies of PSS by 15–20%;
- the presence of LM on PSS does not change the character of deformation and reduces the values of oscillation frequencies by 14–15%, while ruffled loaded PSS have frequencies 15.6–19.8% higher than the basic ones;
- the obtained natural frequency values for ruffled unloaded and loaded PSS significantly exceed the frequency of external disturbance – vibration of typical separating equipment, which indicates the absence of resonance.

Experimental identification of the natural frequencies of cylindrical PSS was conducted according to the methodology described before, and the results are presented in Table 5. The relative error of the results was determined by the formula: $\Delta = (\omega_{ab} - \omega_{ex}) / \omega_{ab} \cdot 100\%$, where ω_{ab} , ω_{ex} – the natural oscillation frequencies of PSS, obtained numerically in Abaqus_CAЕ and experimentally, respectively.

The experimental data demonstrates a sufficient (for practical purposes) agreement with the results of numerical modeling regarding the spectrum of the natural frequencies and oscillation modes (with an average discrepancy of

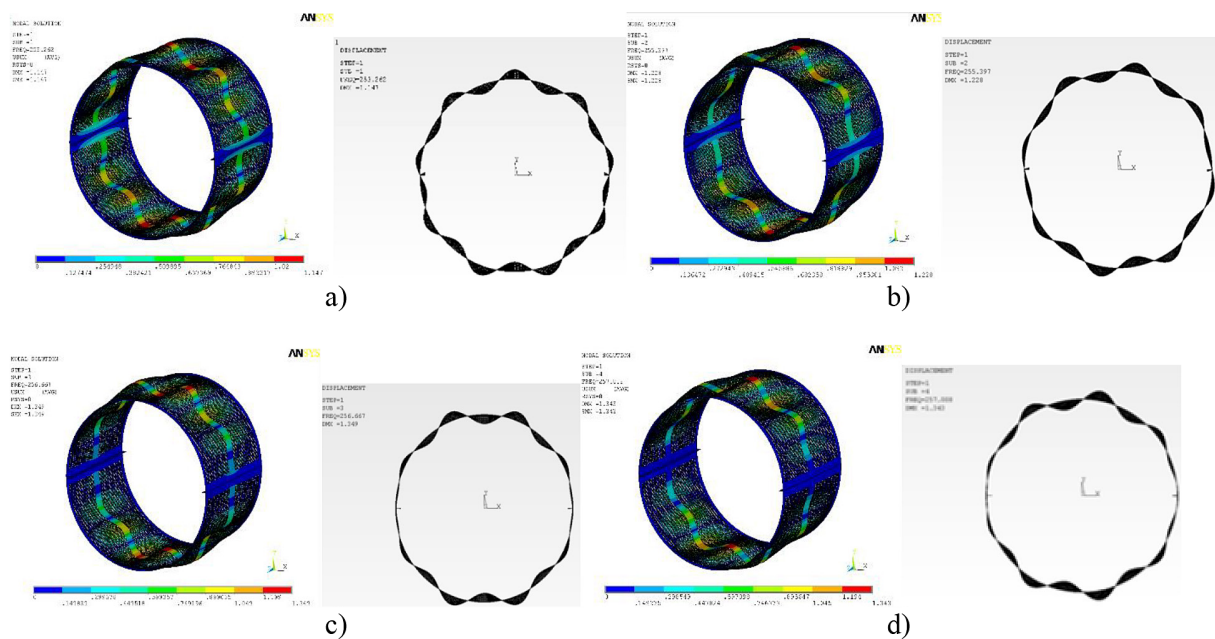


Fig. 12. Modes of PSS oscillations: (a) No. 1; (b) No. 2; (c) No. 3; (d) No. 4

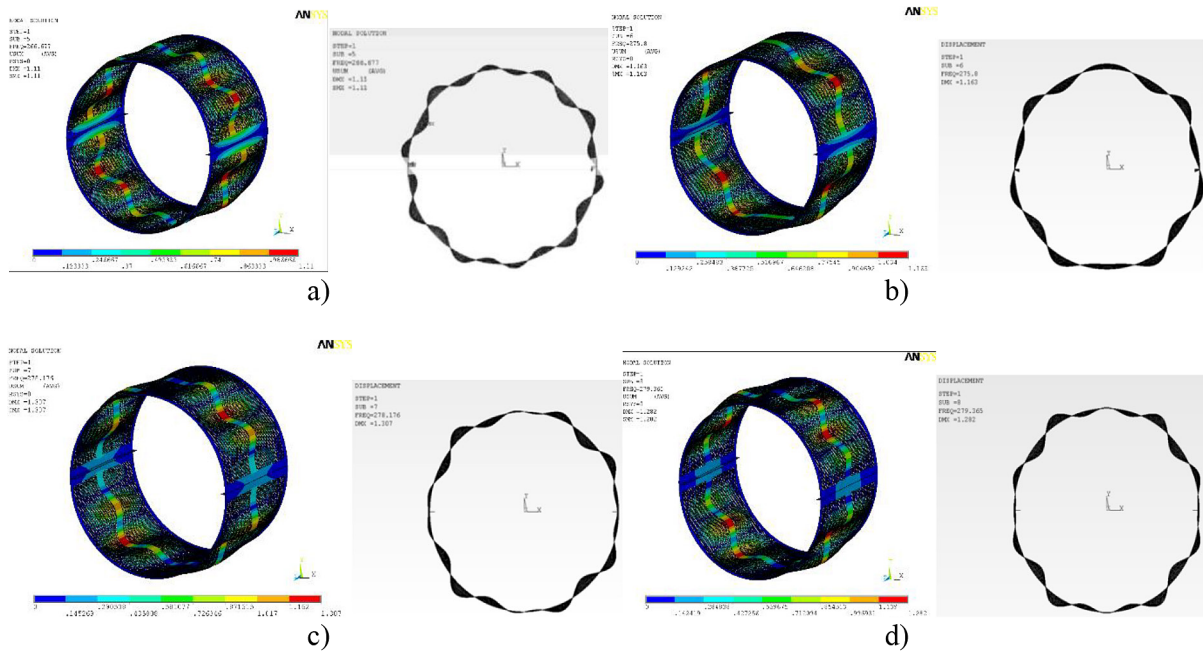


Fig. 13. Modes of PSS oscillations: (a) No. 5; (b) No. 6; (c) No. 7; (d) No. 8

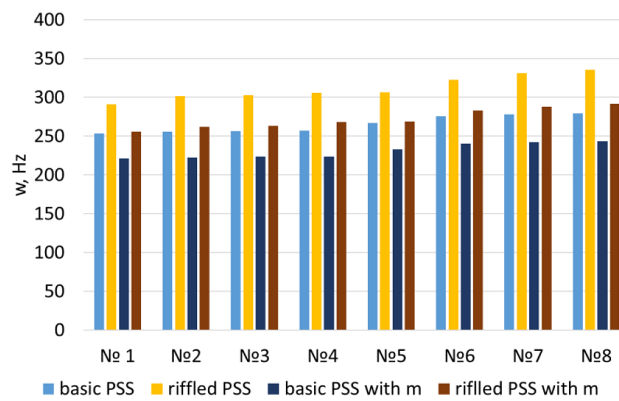


Fig. 14. The natural oscillation frequency of cylindrical PSS at different modes

Table 4. Natural frequencies of PSS oscillations (Hz)

Type of cloth	Attached load	Modes							
		No. 1	No. 2	No. 3	No. 4	No. 5	No. 6	No. 7	No. 8
Base with rectangular holes	without material	253.3	255.5	256.7	257.0	266.7	275.8	278.2	279.4
	with material	220.9	222.5	223.6	223.8	233.1	240.3	242.3	243.3
Riffled with rectangular holes	without material	291.30	301,49	302.91	305.83	306,71	322.69	331.06	335.28
	with material	255.52	262.17	263.40	268.27	269.04	283.06	287.88	291.55

Table 5. The natural oscillation frequency of PSS

Indicators	Mode							
	No. 1	No. 2	No. 3	No. 4	No. 5	No. 6	No. 7	No. 8
PSS with ruffles								
ω_{ab} , Hz	291.3	301.5	302.9	305.8	306.7	322.7	331.1	335.3
ω_{ex} , Hz	277.2	286.8	290.1	292.5	293.7	308.3	322.6	329.2
Δ , %	4.84	4.87	4,23	4.36	4.24	4.46	2.56	1.81
Basic PSS (unriffled)								
ω_{ab} , Hz	253.3	255.3	256.7	257.0	266.7	275.8	278.2	279.4
ω_{ex} , Hz	240.6	242,8	247.2	248.3	256.6	267.6	267.3	271.6
Δ , %	5	4,90	3.70	3.39	3.79	2.97	3.92	2.79

approximately 3.92% for rifflled PSS and 3.81% for basic ones).

This confirms the adequacy of the numerical model and indicates the location of the angular rotation velocity of the rotor of the centrifugal separator $\omega_1 \approx 12s^{-1}$ (1.9 Hz) in the pre-resonance zone, far from the lower natural frequencies of PSS. Use of FE methods and experimental studies made it possible to identify the frequencies of natural oscillations and quantify the difference for different structural and kinematic parameters of structures. The developed technique is universal and, if necessary, can be used for perforations with other hole shapes and parameters.

CONCLUSIONS

Based on the obtained results, the following conclusions were presented:

1. The methodology has been developed to assess the technological efficiency and reliability of cylindrical PSS.
2. A mathematical model of the dynamics of LM along cylindrical sifting surface has been developed, which takes into account the structural and kinematic parameters of PSS, including the shape and parameters of volumetric ruffles, and the properties of LM.
3. Regularities of changes in the dynamic viscosity coefficient of LM subjected to vibration have been obtained, which is significant and comprehensively determines the dynamic characteristics during the sifting of components.
4. Numerical solution of analytical expressions obtained dependences of velocity of corn (sunflower) LM movement and productivity of cylindrical PSS by using rectangular, triangular and oval profile ruffles, their ranges of variation were established.
5. Application of FEM method and experiments allowed to obtain the influence of material and construction properties on the spectrum of frequencies and forms of the natural oscillations of cylindrical rifflled sifting surfaces. Ranges of variation in the oscillation frequencies of cylindrical sifting surfaces have been established, the value of which increases when rifflled structures are used and decreases when they are loaded with LM.
6. The obtained natural frequency values of rifflled cylindrical sifting surfaces significantly exceeds the frequency of external disturbance

– vibration of typical separating equipment, which indicates the absence of resonance.

7. The conducted research will enhance the separation efficiency of LM components on PSS, to provide their reliability and durability, to improve technical and economic indicators of separating equipment.

Acknowledgments

The authors acknowledge the financial support of the National Science Centre in Krakow to the research project funded in the “POLONEZ BIS 2” call No. 2022/45/P/ST8/02312 entitled Numerical-experimental analysis of a sieve holes’ shape and arrangement effect on the degree. POLONEZ BIS is operated by the Centre on the basis of the Grant Agreement No. 945339 concluded with the European Research Executive Agency.

REFERENCES

1. Hou J, Liu X, Zhu H, Ma Z, Tang Z, Yu Y, Jin J, Wang W. Design and Motion Process of Air-Sieve Castor Cleaning Device Based on Discrete Element Method. *Agriculture* 2023; 13: 1130. <https://doi.org/10.3390/agriculture13061130>.
2. Jesny S, Prasobh G.R. A Review on Size Separation. *International Journal of Pharmaceutical Research and Applications* 2022; 7(2): 286-296. <https://doi.org/10.35629/7781-0702286296>.
3. Honghai Liu, Jie Jia, Nieyangzi Liu, Xiaojin Hu, Xiong Zhou. Effect of material feed rate on sieving performance of vibrating screen for batch mixing equipment. *Powder Technology* 2018; 338: 898-904. <https://doi.org/10.1016/j.powtec.2018.07.046>.
4. Bakum M, Kharchenko S, Kovalyshyn S, Krekot M, Kharchenko F, Shvets O, Kielbasa P, Miernik A. Identification of parameters of the separation process of safflower seed material on sieves. *Journal of Physics: Conference Series* 2022, 2408, 012013, IOP Publishing. <https://doi.org/10.1088/1742-6596/2408/1/012013>.
5. Tishchenko L. Intensification of grain separation: monograph. Kharkiv: Osnova, 2004, pp. 224.
6. Kharchenko S. Intensification of grain sifting on flat sieves of vibration grain separators: monograph; Dissa Plus: Kharkiv, 2017, pp. 217.
7. Tabakovic M, Simić M, Stanisavljevic R, Mili-vojevic M, Poštić D. Effects of shape and size of hybrid maize seed on germination and vigour of different genotypes. *Chilean journal of agricultural research*. 2020, 80: 381–392. <https://doi.org/10.4067/S0718-58392020000300381>.

8. Graven L, Carter P. Seed Size/Shape and Tillage System Effect on Corn Growth and Grain Yield. *Journal of Production Agriculture* 1990, 3: 445–452. <https://doi.org/10.2134/jpa1990.0445>.
9. Ovuka J, Crnobarac J, Radic V, Dušanić N, Miklic V. Influence of seed size grade on sunflower plant high. 19th International Sunflower Conference 2016, Edirne, Turkey: 959-964.
10. Adebisi M, Kehinde T, Salau A, Okesola L, Porbeni J, Esuruoso A, Oyekale K. Influence of different seed size fractions on seed germination, seedling emergence and seed yield characters in tropical soybean (*Glicine max L. Merrill*). *International Journal of Agricultural Research* 2013, 8(1): 26–33.
11. Tishchenko L. Hydrodynamic characteristics of fluidised bulk solids at vibrocentrifugal separation at grain processing enterprises. Modern directions of technology and mechanisation of processes of processing and food production: *Bulletin of KhNTUA* 2001, Kharkiv, 5: 13–33.
12. Khizhnikov A. Intensification of grain cleaning process on a cylindrical sieve: *Dissertation Candidate of Technical Sciences: 05.20.01, Barnaul, 2011, pp. 163.*
13. Vasilkovsky M. Increasing efficiency of grain separation on the fast-rotating cylindrical sieve. *Ph.Voronezh, 1987, pp. 24.*
14. 14. Kharchenko S, Kovalyshyn S, Zavgorodniy A, Kharchenko F, Mikhaylov Y. Effective sifting of flat seeds through sieve. *INMATEH-Agricultural Engineering* 2019, 58 (2): 17–26. <https://doi.org/10.35633/INMATEH-58-02>.
15. Piven M. Justification of grain mixture separation process by flat vibrating sieves. *MOTROL. Commission of Motorization and Energetics in Agriculture* 2015, 17 (7), 163–169.
16. Kharchenko S, Kharchenko F, Zarovnyi R. Correction of technological productivity of grain and seed cleaning machines *Proceedings of the III International Scientific and Practical Internet Conference “INNOVATIONS: Theory and practice”*. Kropyvnytskyi: Academy of Applied Sciences. 2022, pp. 32-34.
17. Krzysiak Z, Samociuk W, Zarajczyk J, Kaliniewicz Z, Pieniak D, Bogucki M. Analysis of the Sieve Unit Inclination Angle in the Cleaning Process of Oat Grain in a Rotary Cleaning Device. *Processes* 2020, 8: 346. <https://doi.org/10.3390/pr8030346>.
18. Manoach E, Warminski J, Mitura A. et al. Dynamics of a laminated composite beam with delamination and inclusions. *Eur. Phys. J. Spec. Top.* 2013, 222: 1649–1664. <https://doi.org/10.1140/epjst/e2013-01952-6>.
19. Kharchenko S, Samborski S, Kharchenko F, Paśnik J, Kovalyshyn S, Sirovitskiy K. Influence of Physical and Constructive Parameters on Durability of Sieves of Grain Cleaning Machines. *Advances in Science and Technology Research Journal* 2022, 16 (6): 156-165.
20. Samborski S, Korzec I. Application of the Acoustic Emission Technique for Damage Identification in the Fiber Reinforced Polymer Composites. *Advances in Science and Technology – Research Journal* 2023, 17(1): 210-221. <https://doi.org/10.12913/22998624/156602>.
21. Ciecieląg K, Kęćik K, Skoczylas A, Matuszak J, Korzec I, Zaleski R. Non-destructive detection of real defects in polymercomposites by ultrasonic testing and recurrence analysis. *Materials* 2022, 15(20): 7335.
22. Voloshin M. On analogies in the kinematic modes of flat and centrifugal-vibrating sieves of grain machines. *Mechanization and electrification of agriculture* 1995, 81: 37-40.
23. Kharchenko S, Samborski S, Kharchenko F, Kotliarevskiy I. Determination of Hole Blocking Conditions for Perforated Sifting Surfaces. *Advances in Science and Technology Research Journal.* 2024; 18(5): 342-360. <https://doi.org/10.12913/22998624/190483>.
24. Tishchenko L. Rational cleaning of vertical vibrocentrifugal grids. *Mechanization and electrification of agriculture* 1984, 2: 52-55.
25. Tishchenko L, Kharchenko S, Kharchenko F, Bredykhin V, Tsurkan O. Identification of a mixture of grain particle velocity through the holes of the vibrating sieves grain separators. *East. Eur. J. Enterp. Technol.* 2016, 2: 63–69. <https://doi.org/10.15587/1729-4061.2016.65920>.
26. Tishchenko L, Olshansky V, Olshansky S. *Hydrodynamics of grain separation: monograph.* Kharkiv: Miskdruk., 2010, 174 p.
27. Lukyanenko V. Choice of continuum dynamics model to describe vibration separation processes of seed mixtures. *MOTROL. Commission of Motorization and Energetics in Agriculture* 2015, 17 (7): 3–10.
28. Giani S, Hakula H. Free vibration of perforated cylindrical shells of revolution: Asymptotics and effective material parameters. *Computer Methods in Applied Mechanics and Engineering* 2023, 403A: 115700. <https://doi.org/10.1016/j.cma.2022.115700>.
29. Kalamkarov A, Andrianov I, Weichert D. Asymptotic analysis of perforated shallow shells. *Internat. J. Engrg. Sci.* 2012, 53: 1-18.
30. Kharchenko S, Samborski S, Kharchenko F, Mitura A, Paśnik J, Korzec I. Identification of the Natural Frequencies of Oscillations of Perforated Vibrosurfaces with Holes of Complex Geometry. *Materials* 2023; 16: 5735. <https://doi.org/10.3390/ma16175735>.
31. Gan Tang, Ping Sun, Yanqi Zhao, Lingfeng Yin and Hong Zhuang. Experimental research on friction coefficient between grain bulk and bamboo clappers. *IOP Conf. Series: Materials Science*

- and Engineering 2017, 274: 012116. <https://doi.org/10.1088/1757-899X/274/1/012116>.
32. Mudasir A, Charanjiv S, Fatih Y. Engineering properties of sunflower seed: Effect of dehulling and moisture content. *Cogent Food & Agriculture* 2016, 2(1). <https://doi.org/10.1080/23311932.2016.1145783>.
33. Mazorenko D. Improving the efficiency of vibration centrifugal separators by determining their rational schemes and parameters. *Vibrations in engineering and technology* 2003, 6(32): 3–12.
34. Tishchenko L, Piven M, Kharchenko S, Bredikhin V. Investigation of the regularities of vibration resistance of grain mixtures during separation by cylindrical vibrocentrifugal sieves. *Modern directions of technology and mechanisation of processes of processing and food production. Bulletin of KhNTUA* 2009, 88: 34–44.
35. <https://frunze.ua/instruktsii/tipy-perforatsii/tip-2a-pryamougolnye-otverstiya-raspolozhennye-ryadami/>
36. Tishchenko L. To determination of hydrodynamic characteristics of fluidized bulk solids during operation of vibrocentrifugal separators. *Ecology and agricultural machinery. Collection of scientific works*. 2000, Vol. 1: 70–73.
37. Tishchenko L. Determination of dynamic characteristics of the cylindrical screen blade on the basis of finite-element models. *Scientific articles of NAU* 2003, 60: 315–323.
38. Tishchenko L, Abdueva F, Olshansky V. Comparison of two methods of determining the coefficient of viscosity of the freeze-dried grain mixture at vibration-centre separation. *Vibrations in technology and engineering* 2008, 1(50), 96–100.
39. Lurie A.I. *Theory of Elasticity*. M.: Nauka, 1970, pp. 940.
40. Norrie D., de Fries J. *Introduction to the Finite Element Method*. M.: Mir, 1981, pp. 304.
41. Strang G., Fix J. *Theory of the finite element method*. M.: Mir, 1977, pp. 349.
42. Wilkinson J.H. *The algebraic problem of eigenvalues*. M.: Nauka, 1970, pp. 564.
43. *Vibrations in Engineering: Handbook in 6 vols*. M.: Mashinostroenie, 1981, Vol. 5: Measurements and tests, pp. 496.